



Targeting GRP receptor: Design, synthesis and preliminary biological characterization of new non-peptide antagonists of bombesin

Alessandro Palmioli^{a,b}, Gabriella Nicolini^{b,c}, Farida Tripodi^a, Alexandre Orsato^{a,d}, Cecilia Ceresa^{b,c}, Elisabetta Donzelli^{b,c}, Martina Arici^a, Paola Coccetti^a, Marcella Rocchetti^a, Barbara La Ferla^{a,*}, Cristina Airoidi^{a,b,*}

^a Department of Biotechnology and Biosciences, University of Milano - Bicocca, P.zza della Scienza 2, 20126 Milan, Italy

^b Milan Center for Neuroscience, University of Milano-Bicocca, P.zza dell'Ateneo Nuovo 1, 20126 Milano, Italy

^c School of Medicine and Surgery, Experimental Neurology Unit, University of Milano - Bicocca, Via Cadore 48, 20900 Monza, MB, Italy

^d Departamento de Química, CCE, Universidade Estadual de Londrina, CEP 86057-970 Londrina, Paraná, Brazil

ARTICLE INFO

Keywords:

Gastrin Releasing Peptide (GRP)
GRP receptors (GRP-R)
Bombesin (BN)
Circular dichroism
NMR-based structural and conformational analysis
MM and MD conformational studies
GRP-R antagonists
GRP-R ligands

ABSTRACT

We report the rational design, synthesis, and *in vitro* preliminary evaluation of a new small library of non-peptide ligands of Gastrin Releasing Peptide Receptor (GRP-R), able to antagonize its natural ligand bombesin (BN) in the nanomolar range of concentration.

GRP-R is a transmembrane G-protein coupled receptor promoting the stimulation of cancer cell proliferation. Being overexpressed on the surface of different human cancer cell lines, GRP-R is ideal for the selective delivery to tumor cells of both anticancer drug and diagnostic devices. What makes very challenging the design of non-peptide BN analogues is that the 3D structure of the GRP-R is not available, which is the case for many membrane-bound receptors. Thus, the design of GRP-R ligands has to be based on the structure of its natural ligands, BN and GRP.

We recently mapped the BN binding epitope by NMR and here we exploited the same spectroscopy, combined with MD, to define BN conformation in proximity of biological membranes, where the interaction with GRP-R takes place. The gained structural information was used to identify a rigid C-galactosidic scaffold able to support pharmacophore groups mimicking the BN key residues' side chains in a suitable manner for binding to GRP-R.

Our BN antagonists represent hit compounds for the rational design and synthesis of new ligands and modulators of GRP-R. The further optimization of the pharmacophore groups will allow to increase the biological activity. Due to their favorable chemical properties and stability, they could be employed for the active receptor-mediated targeting of GRP-R positive tumors.

1. Introduction

Peptide receptors have been shown to be over-expressed in several types of human neoplasia [1,2]. These observations have led to the development of diagnostic and radio-therapeutic applications, using radiolabeled peptides for *in vivo* receptor scintigraphy or peptide radiotherapy [3] in tumor patients. Furthermore, peptides linked to cytotoxic drugs [4] or stable peptide agonists or antagonists [5,6] have been used for long-term targeted chemotherapy in animal tumor models.

Bombesin (BN), a 14 amino acid (Pyr-QRLGNQWAVGHLN-NH₂) peptide isolated in amphibians, and its mammalian counterpart gastrin-

releasing peptide (GRP) [7], a 27 amino acid peptide that shares the same C-terminal decapeptide with BN with the exception of one amino acid, are hormonally active peptides that function as autocrine or paracrine growth factors in a variety of cells. Their sequence homology accounts for an identical physiological action, triggered by the ability to interact with the same receptors.

BN/GRP receptors (GRP-R) are G-protein coupled receptors (GPCR) involved in several biological processes. The binding of BN/GRP to their cognate receptors leads to a rapid intracellular calcium mobilization from internal stores [8,9], as well as to the activation of multiple transduction pathways, which act synergistically to promote cell

* Corresponding authors at: Department of Biotechnology and Biosciences, University of Milano - Bicocca, P.zza della Scienza 2, 20126 Milan, Italy (C. Airoidi).
E-mail addresses: barbara.laferla@unimib.it (B. La Ferla), cristina.airoidi@unimib.it (C. Airoidi).

proliferation [8]. For this reason, these receptors play an important role in cancer development and are frequently over-expressed in many human tumors [1]. The involved growth mechanisms and the possible therapeutic potential have been well studied in the case of GRP-R, particularly in lung, prostate and head/neck cancer cells. This evidence suggests GRP-R as a very good marker of carcinogenesis and possible target for receptor-mediated tumor targeting [10].

By preventing the receptor activation, GRP-R antagonists could have a powerful application as potential anticancer compounds [11,12]. On the other hand, GRP-R agonists can be a powerful tool for the development of new tumor targeting strategies. In a mechanism that is typical for GPCR, the GRP-R is internalized by endocytosis after binding to agonists [13]. This feature can be exploited to promote the selective internalization of cytotoxic drugs by tumor cells over-expressing GRP-R, through the chemical conjugation of anticancer agents with GRP-R agonists. However, also receptor antagonists, when showing a high affinity for the target, can be exploited to deliver selectively cytotoxic drugs at the tumor site, providing therapeutic effects [14,15]. High affinity GRP-R ligands, independently of their putative agonistic/antagonistic activity, can also deliver diagnostic tools at the tumor site [16].

Notably, the use of GRP-R natural ligands GRP and BN as peptide carriers for tumor targeting and/or therapy is anyway a very limited strategy, because of their low metabolic stability [17–19]. Thus, the design of synthetic and chemically stable GRP/BN analogues presenting agonist/antagonist activities, and, possibly, also an increased affinity for the receptor is of paramount importance.

Both GRP-R agonists and antagonists have been reported [17–19], but these compounds are essentially peptide-pseudopeptide in nature, and, consequently, due to the presence of amide bonds, proteolytically unstable under physiological conditions. This evidence prompted the search for GRP-R non-peptide ligands. Nevertheless, the only non-peptide antagonist is the compound PD176252 and its derivatives; however, it has poor selectivity, due to its excessive conformational flexibility [20,21].

What makes very challenging the design of non-peptide BN analogues is that the three-dimensional structure of the GRP-R is not available, which is the case for many membrane-bound receptors. Thus, the design of GRP-R ligands must be based on the structure of its natural ligands, BN and GRP. For this reason, we recently exploited advanced Nuclear Magnetic Resonance (NMR) spectroscopy techniques to study the binding of BN to GRP-R, identifying the structural determinants of this interaction [22]. Saturation Transfer Difference (STD) NMR experiments acquired on samples containing BN and tumor cells expressing the receptor on their surface afforded high-quality spectra, allowing the identification of Trp and His belonging to the C-terminal fragment of the peptide among the most important for GRP-R recognition and binding [22].

Moreover, in this paper we combined Nuclear Overhauser Effect Spectroscopy (NOESY) experiments and molecular dynamic (MD) simulations verifying the propensity of BN to adopt an α -helix conformation in proximity of the cell membrane.

Hence, starting from the structural information gained, we designed a small library of GRP-R potential ligands.

To this end, we exploited a carbohydrate scaffold, already reported by our group [23], functionalizable at four different positions, with as many pharmacophore groups. The cyclic structure of carbohydrates, characterized by several hydroxyl groups presenting specific spatial orientations, can be indeed properly functionalized for the generation of libraries of compounds by the combinatorial decoration with different pharmacophores [24–26]. Moreover, at variance with peptides, compounds based on scaffolds from carbohydrate-derivatives, for example C-glycosides, have a high chemical and metabolic stability and a poor conformational flexibility, allowing to increase ligands' affinity and selectivity for the receptor.

The ability of the selected C-glycidic scaffold to bear the putative pharmacophores properly oriented in space for the interaction with

GRP-R was assessed by molecular mechanics (MM) and molecular dynamics (MD) simulations.

After their synthesis, compounds were preliminary evaluated for their ability to act as agonists or antagonists of the receptor.

2. Results and discussion

2.1. Bombesin conformational analysis

BN conformation has been studied in various solvents, demonstrating that it adopts an unordered structure in aqueous media and in dimethyl sulfoxide [27], while a helical structure has been observed in aqueous solutions containing trifluoroethanol (TFE) [28] or membrane mimetics [29,30]. To deepen this point, we applied circular dichroism (CD) and NMR spectroscopy to characterize BN conformational behavior in presence of sodium dodecyl sulphate (SDS) micelles, a biological membrane mimetic [31] recently employed for the study of its effect on neuromedin C (NMC) conformation [32].

First, we performed a CD analysis of BN and BN (8-14), the minimal carboxyl fragment interacting with the receptor, acquired in absence or presence of SDS micelles (Supporting information - Figure S1). The CD spectra of BN and BN (8-14), acquired in an aqueous solution, indicate that in this condition the peptides are disordered, as evidenced by the minimum located at 197 nm (Supporting information - Figure S1, blue, red and green spectra) [33].

However, in both cases the addition of 150 mM SDS [32] induced a conformational change characterized by a notable increment of the α -helical content and a decrement of random coil regions, as indicated by the positive band around 190 nm and the increase of the negative ellipticities around 206 and 220 nm (Supporting information - Figure S1, violet, yellow, black spectra). This behavior was independent from temperature, as experiments collected at 10, 25 and 37 °C gave overlapping spectra. These results, in agreement with previous studies performed in presence of membrane mimetics, indicate that both peptides adopt a predominant α -helix conformation upon addition of SDS micelles, at all the three tested temperatures.

Accordingly, NMR spectroscopy also supported this conformational change. The direct comparison of ^1H NMR (Supporting information - Figure S2) and 2D-NOESY (Supporting information - Figure S3) spectra acquired in absence (A) or presence (B) of 150 mM d_{25} -SDS at pH 7.0, 25 °C, reveals dramatic differences. Analogous results were obtained when experiments were performed at 10 or 37 °C (data not shown). In fact, the inter-residual NOE connectivity in the fingerprint region of NOESY spectra (Supporting information - Figure S3) suggested an unordered (Supporting information - Figure S3-A) vs a folded (Supporting information - Figure S3-B) conformation of the peptide. The ^1H and ^{15}N NMR assignments (Supporting information - Table S1) were exploited to calculate the solution structures of BN in presence of SDS micelles. The secondary structure and RCI-S2 prediction window suggested the involvement of all BN residues in a α -helix secondary structure (Supporting information - Figure S4). NOEs intensities were used as geometrical restraints during the simulated annealing molecular dynamics (SA-MD) calculations performed through the CYANA software [34,35]. As reported in Fig. 1A, the corresponding BN structure obtained in presence of the membrane mimetic resembles an α -helix. The tridimensional structure is freely available as .pdb files on Mendeley Data repository [36].

The same conformational behavior was recently described for neuromedin C (NMC) [32], an endogenous decapeptide (GNHWAVGHLN-NH₂) highly conserved in mammals that exerts a variety of biological effects both on the central nervous system (CNS) and in the gastrointestinal tract [37], belonging to the bombesin-like peptide family. As confirmation, BN and NMC conformations obtained in presence of SDS micelles present a significant overlap (Fig. 1B) showing the same arrangement both of the backbone and of the side chains of the amino acids important for the binding to the receptor (Trp8, His12 and Leu13

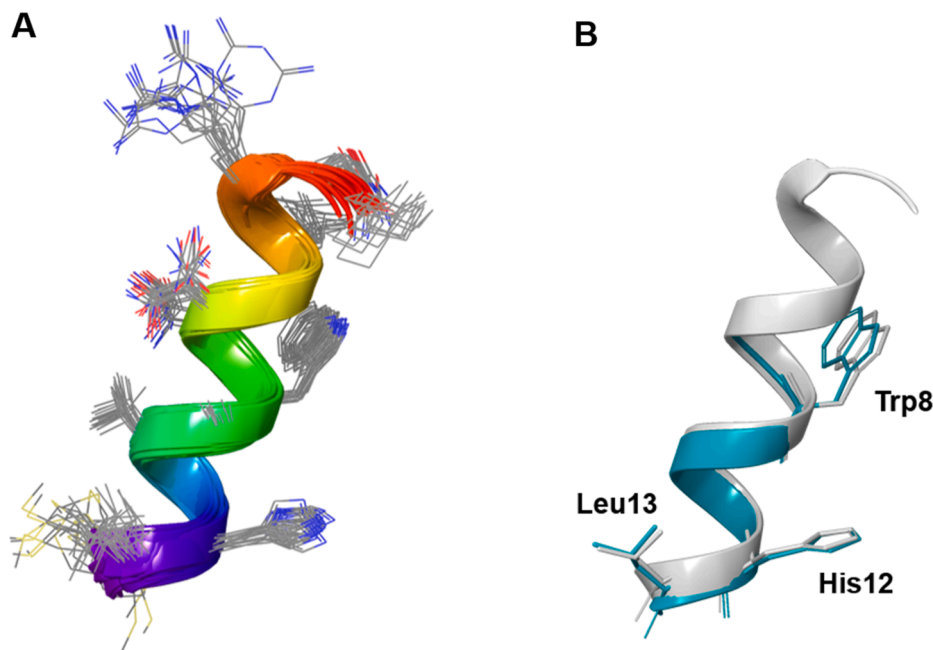


Fig. 1. (A) Bundle of the 10 best BN conformers calculated through CYANA from NOESY conformational restrains obtained in presence of SDS micelles. (B) Superimposition of BN and NMC structures [32] (one conformer for each) both calculated in presence of SDS micelles.

in BN [22].

2.2. GRP-R ligands design and synthesis

The rational design of the non-peptidic BN-like compounds was based on the analysis of BN conformation in SDS micelles solution, supporting its α -helical conformation (Fig. 1A) in proximity of biological membranes, where the interaction with GRP-R takes places, and the BN binding epitope recently reported by our group [22], indicating the involvement of residues Trp8, His12, Leu13 and, with a lower extent, Met14 side chains in its molecular recognition of the receptor. These structural data were exploited to design BN analogues based on a rigid scaffold able to spatially orient, in an effective way, the potential pharmacophores, as putative mimetics of the side chains of BN aminoacids mainly involved in the binding to GRP-R.

To this end, we evaluated the use of different glycidic scaffolds deriving from natural sugars and their more stable derivatives (eg, C-glycosides) [38]. We selected the scaffold depicted in Fig. 2, presenting four different possible sites of functionalization and already described by our group [23]. This scaffold was used to design a small library of compounds, reported in Fig. 2, bearing the putative pharmacophores properly oriented in space.

The proper pharmacophores' orientation was supported by the conformational analysis made on compound GRPR-L3 and carried out using molecular mechanics (MM) and molecular dynamics (MD) simulations. Calculations were performed by using AMBER* force field [39], as implemented in the MacroModel program (Schrödinger Suite) [40] (Supporting information - Figure S5A). Then the relative spatial arrangement of GRPR-L3 pharmacophores was compared with that of Trp8, His12 and Leu13 side chains in BN structure as calculated in

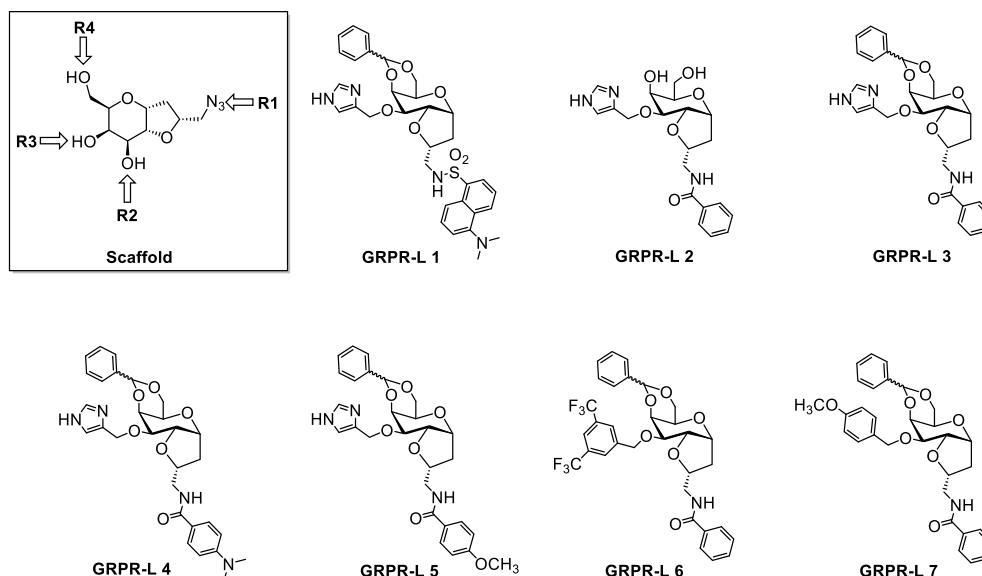


Fig. 2. Structures of the bicyclic C-galactosidic scaffold, with indication of the four (R1, R2, R3 and R4) and the putative GRPR ligands (GRPR-L) 1–7.

presence of membrane mimetic (Fig. 1A and B). Fig. 3 reports the superimposition of the two structures and clearly shows that the imidazole ring inserted in GRPR-L3 structure as R2 group overlaps with the side chain of BN His12, the aromatic entity introduced as R1 with the indole ring of Trp8, while benzylidene in position R3 and R4 is very closed to the side chains of Leu13, reproducing a hydrophobic environment suitably spaced from the other two groups of the BN binding epitope.

All the GRP-R ligands were prepared from the rigid bicyclic C-galactosidic scaffold bearing a furan ring fused to the C1-C2 bond of the sugar moiety, substituted with an azido-methylene group with an (*R*) configuration on C8 (compound 4(*R*)). The synthesis of 3, as a mixture of diastereoisomers at C8, is easily achievable from commercially available methyl- α -D-galactopyranoside and has been previously reported [23]. The regioselective introduction of a benzylidene group on C4 and C6 hydroxyls allowed the separation of the two diastereoisomers affording the core structure, starting material for the synthesis of the GRPR ligands library (Scheme 1).

The synthesis of a first set of ligands (GRPR-L1, 3, 4, 5) containing two common pharmacophoric entities, the 4-6 *O*-benzylidene moiety and the imidazole group on C3-OH, and bearing different amide derivatives, is described in Scheme 2.

Intermediate 4(*R*) was successfully alkylated at C3-OH with a trityl protected imidazole [41] (5, NaH, THF/DMF) with acceptable yields (77%, compound 6), attempts with differently protected imidazole moieties such as BOC and Cbz did not lead to the desired alkylation

product but instead basic reaction conditions lead to the transfer of the protective group from the imidazole to the sugar C3-OH. The azide was then selectively reduced through catalytic hydrogenation (H_2 , Pd Lindlar), and the obtained amine 7 was acylated with different aromatic acyl-chlorides to afford the protected ligands compounds 8, 9, 10, 11 in high yields. Removal of the trityl protection in mild acidic conditions (5% HCOOH in MeOH) afforded GRPR-L1, 3, 4, 5. Compound 9 was also deprotected from the benzylidene moiety (TFA 50%), in order to afford GRPR-L2, containing only two pharmacophoric groups.

The second set of GRP-R ligands (GRPR-L6 and 7) (Scheme 3) are analogues of GRPR-L3 but carry a different pharmacophoric group on the C3-OH.

The groups were selected in order to verify the importance of the imidazole entity and to simultaneously explore the possibility to introduce detectable groups/elements that could be exploited by diagnostic techniques such as fluorinated groups (CF_3) that can be easily detected by NMR. Compound 4(*R*) was alkylated at C3-OH with different benzyl halide derivatives (NaH, THF/DMF), affording compounds 12–14 with good yields. These were then converted to the final ligands GRPR-L6 and L7 through reduction of the azido group followed by reaction with benzoyl chloride.

2.3. Screening and biological evaluation of new GRP-R ligands.

Compounds presenting three pharmacophoric groups, and therefore

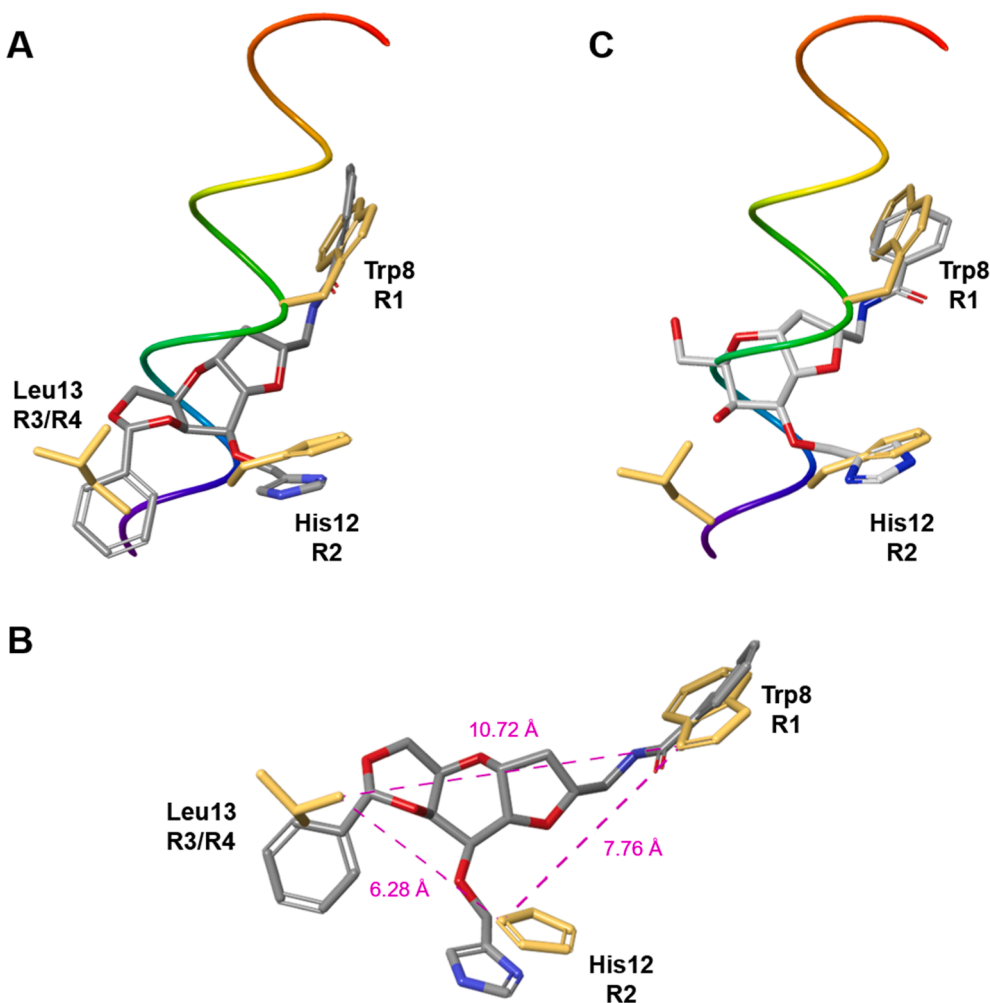
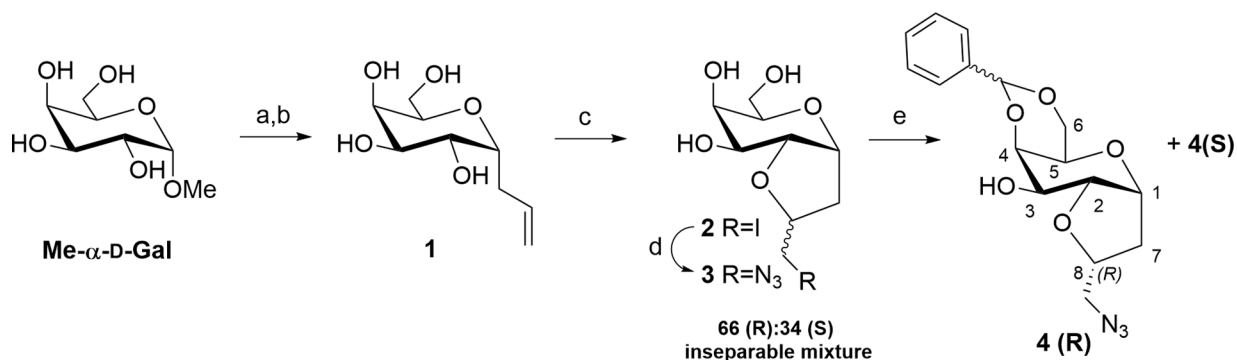
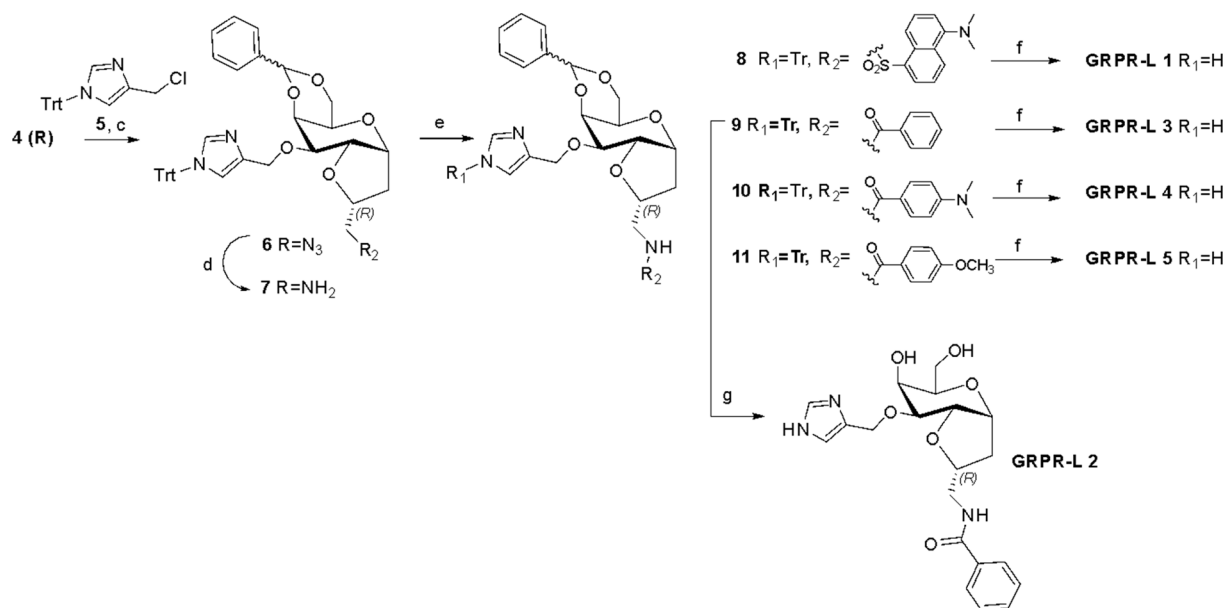


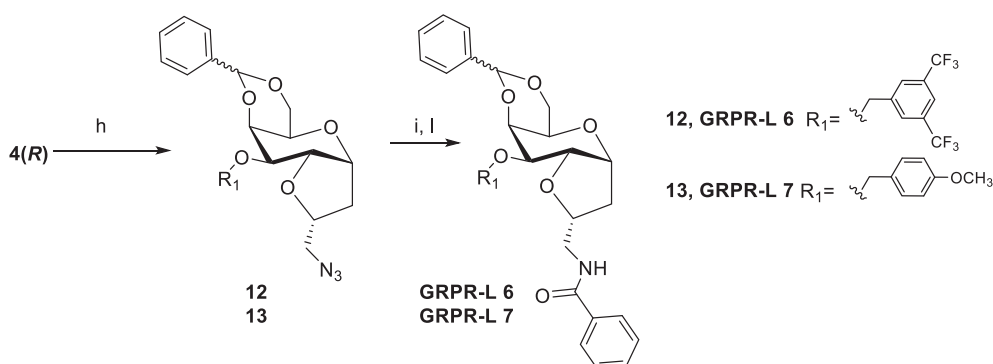
Fig. 3. (A) Superimposition of BN structure calculated in presence of SDS micelles and GRPR-L3 structure obtained through MM and MD calculations; (B) Distances among BN Trp, His and Leu residues involved in GRP-R binding and their overlap with R1, R2 and R3/R4 putative pharmacophores in GRPR-L3 structure; (C) Superimposition of BN structure calculated in presence of SDS micelles and GRPR-L2 structure obtained through MM and MD calculations.



Scheme 1. Synthesis of intermediate **4(R)**, used as scaffold template: (a) BSTFA, MeCN dry, reflux, 1 h then (b) Allyl-TMS, TMSOTf rt, O.N. 74%; (c) NIS, DMF dry, 78%; (d) NaN₃, DMF dry, quant %; (e) benzaldehyde dimethyl acetal, CSA, DMF dry, 70 °C, in vacuo, 75%, 48%(R) + 27% (S).



Scheme 2. Synthesis of **GRPR-L 1–5**: (c) NaH, THF/DMF dry O.N. rt, 77%; (d) H₂, Pd Lindlar, MeOH deg then e) Et₃N, DCM dry; Dansyl-Cl, 92% (**8**); BzCl, 98% (**9**); 4-(Dimethylamino)benzoyl chloride, 87% (**10**); 4-Methoxybenzoyl chloride, 88% (**11**) (f) HCOOH 5%, MeOH dry, 50 °C; 92% (**GRPR-L 1**); quant. yield % (**GRPR-L 3**); 92% (**GRPR-L 4**); 83% (**GRPR-L 5**); g) TFA 50% in MeOH dry, quant. Yield (**GRPR-L 2**).



Scheme 3. Synthesis of **GRPR-L 6, 7**: (h) NaH, THF/DMF dry O.N. rt; 3,5-Bis(trifluoromethyl)benzyl chloride, 73% (**12**); 4-Methoxybenzyl chloride, 87% (**13**); (i) H₂, Pd Lindlar, MeOH deg, then (l) BzCl, Et₃N, DCM dry, 89% (**GRPR-L 6**); 87% (**GRPR-L 7**).

more promising as potential ligands, were screened for their ability to agonize/antagonize BN activity in PC3 (Prostate Cancer) cells, chosen as experimental models because of their GRP-R overexpression [42,43]. We tested their ability to stimulate intracellular Ca²⁺ mobilization, as expected for BN agonist, or decrease BN-induced intracellular Ca²⁺

mobilization, as observed for antagonists. PC3 cells were loaded with the Ca²⁺ sensitive dye Fluo4-AM and intracellular Ca²⁺ mobilization was measured in the presence of each ligand. No compound showed significant agonist activity. However, our compounds showed, although with different efficacy, an antagonistic effect against BN-induced Ca²⁺

mobilization. Fig. 4 reports the increase of Ca^{2+} levels induced by 200 nM BN with or without 30 min pre-treatment with 50 nM test compounds.

As BN binding to GRP-R stimulates cell proliferation, our molecules' ability to counteract this effect was assayed. PC3 cells were treated with 50 nM of the different compounds (GRPR-L) and then with BN to stimulate proliferation. GRPR-L4-7 showed a very potent effect in preventing PC3 BN-induced proliferation (Fig. 5A).

Moreover, to validate the results we performed the same experiment in a second cell model represented by MCF-7 (Michigan Cancer Foundation-7), a breast cancer cell line also characterized by GRP-R overexpression whose proliferation is increased after treatment with BN [44]. Results depicted in Fig. 5B confirmed those observed on PC3 cells except for compound GRPR-L7 whose activity, in this case, was not statistically significant. This evidence fits with the lack of inhibition of BN-induced Ca^{2+} mobilization (Fig. 4) and suggests a different molecular mechanism responsible for GRPR-L7 inhibition of PC3 growth.

Collectively, these preliminary experiments performed to characterize GRPR-L's ability to prevent the BN-induced activation of GRP-R clearly demonstrated that compounds GRPR-L4-6 are able to antagonize both the BN-induced Ca^{2+} mobilization and the BN-induced proliferation of PC-3 and MCF-7 cell lines in the nanomolar range of concentration. These bioactive compounds present three potential pharmacophore groups: a benzylidene moiety in position R3 and R4, an imidazole (GRPR-L4 and L5) or a 3,5-bis-(trifluoromethyl) phenyl (GRPR-L6) group in R2 and a phenyl amide, with or without *para* substituents, in R1 (Fig. 2). These findings support our scaffold ability to orient the pharmacophore groups in an effective way to promote interaction with the receptor mimicking the 3D pharmacophore template of the natural ligands BN and NMC (Fig. 1B).

Moreover, due to the poor water solubility of GRPR-L4-6, we decided to also submit compound GRPR-L2 to proliferation assays on PC3 and MCF-7 cell lines. GRPR-L2 is a synthetic variant devoided of the benzylidene pharmacophore that therefore presents a good solubility in water. Very interestingly, GRPR-L2 showed an ability to counteract the BN-induced cell proliferation comparable to the best inhibitors (Fig. 5). Notably, the superimposition of BN conformation obtained in presence of SDS micelles (Fig. 1) and GRPR-L2 structure as calculated by MM and MD (Supporting information - Figure S5B) showed that also in this case the pharmacophores in R1 and R2 overlap with Trp8 and His12 side chains (Fig. 3C). This evidence suggested that the presence of two aromatic entities on the bicyclic scaffold, mimicking Trp indole and His imidazole rings and oriented in a suitable manner, could be enough to obtain a high affinity for the receptor and a considerable antagonistic activity.

The higher water solubility of compound GRPR-L2, together with the presence of two free hydroxyl groups exploitable for further chemical functionalization, makes also this GRP-R ligand an interesting hit compound for the development of a new library of GRP-R ligand and modulators.

3. Experimental section

3.1. General procedures and materials

BN and BN (8-14) were purchased as lyophilized powders from Bachem AG (Bubendorf, Switzerland). Chemicals were purchased from Sigma Aldrich (St. Louis, MO, US) and Thermo Fisher Scientific (Waltham, MA, US) and used without further purification, unless otherwise indicated. When anhydrous conditions were required, the reactions were performed in oven-dried glassware under argon atmosphere. Anhydrous solvents over molecular sieves were purchased from Acros Organics® (Thermo Fisher Scientific, Waltham, MA, US) with a content of water ≤ 50 ppm. Thin layer chromatography (TLC) was performed on silica gel 60F₂₅₄ plates or RP-C18 Silica plates (Merck Darmstadt, Germany) and visualized with UV detection (254 nm and 365 nm) or using appropriate developing solutions. Flash column chromatography was performed on silica gel 230–400 mesh (Merck KGaA, Darmstadt, Germany), according to the procedure described in the literature. Automated flash chromatography was performed on a Biotage® Isolera™ Prime system (Biotage, Uppsala, Sweden). NMR experiments were recorded on a Varian 400 MHz or a Bruker Avance III 600 MHz equipped with a cryogenic probe instrument at 298 K. Chemical shifts (δ) are reported in ppm downfield from the residual solvent peak, whereas coupling constants (*J*) are stated in Hz. The ¹H and ¹³C NMR resonances of compounds were assigned by means of COSY and HSQC experiments. NMR data processing was performed with MestReNova v14.1 software (Mestrelab Research, Santiago de Compostela, Spain). Mass spectra (ESI-MS) were recorded on a Sciex 3200 Qtrap®.

3.2. BN conformational studies

3.2.1. Circular dichroism (CD)

CD spectra of BN and BN(8–14) were obtained on a Jasco-815 spectropolarimeter equipped with a thermostated cell holder controlled by a Jasco Peltier element (Jasco Europe S.R.L., LC, Italy). Far-UV CD spectra were acquired from 260 to 185 nm at 10, 25 or 37 °C in a 1 mm pathlength quartz cuvette at a BN or BN(8-14) concentration of 75 μM in 10 mM phosphate buffer (pH 7.4) in absence or in presence of 150 mM SDS. The scan speed was 20 nm/min with a response time of

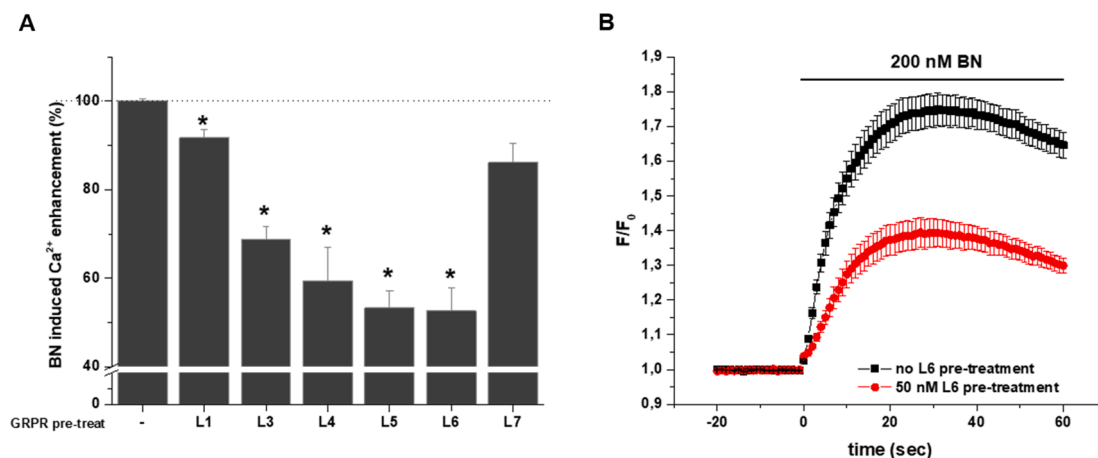


Fig. 4. (A) Intracellular Ca^{2+} mobilization in PC3 cells induced by 200 nM BN with or w/o pre-treatment with 50 nM GRPR-L. **p* < 0.05 vs BN w/o GRPR-L pre-treatment (unpaired *t*-test) (two independent experiments with six replicates). (B) Time dependent changes of BN-induced Ca^{2+} enhancement with (red line) or w/o GRPR-L6 pre-treatment (black line). (For interpretation of the references to colour in this figure legend, the reader is referred to the web version of this article.)

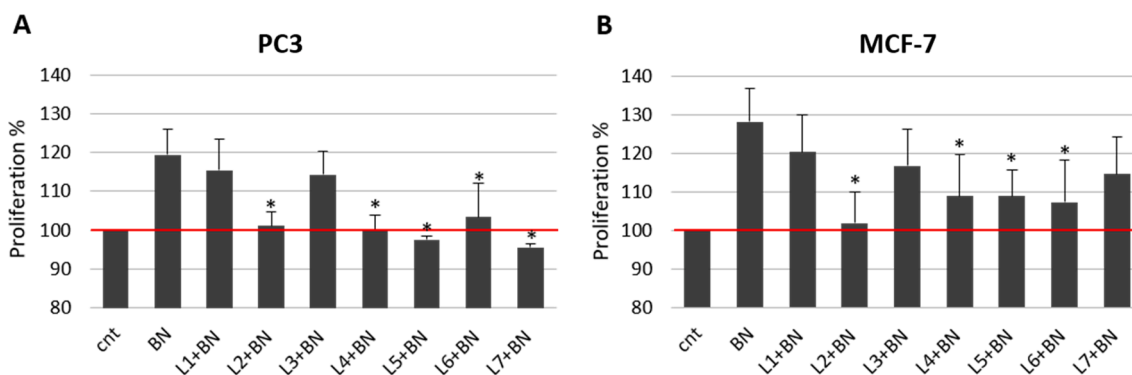


Fig. 5. PC3 and MCF-7 proliferation rate after treatment with BN in the absence or presence of 50 nM of test compounds (GRPR-L). Proliferation assay was performed after 24 h of treatments. * $p < 0.05$ relative to BN treatment.

2 s and a step resolution of 0.2 nm, whereas 3 scans were accumulated. Buffer spectra were subtracted for all spectra.

3.2.2. NMR spectroscopy and SA-MD

NMR experiments in presence of SDS micelles. Samples for the NMR-based conformational studies were prepared by dissolving the peptide in 500 μ L of PB or d_{25} -SDS aqueous solution (9:1 $H_2O:D_2O$, PB buffer at pH 7.0) to make a final BN concentration of 0.7 mM and a SDS final concentration of 150 mM. The NMR spectra were recorded at 10, 25 or 37 $^{\circ}C$ with a Bruker Avance III 600 MHz NMR spectrometer equipped with a 5 mm QCI cryo-probe (Bruker Inc., Billerica, MA, US). 1- and 2D spectra were recorded suppressing water signal by excitation sculpting. For each of these experiments, 512 t1 increments were used. 32, 64 and 96 transients were collected for $^1H, ^1H$ TOCSY, $^1H, ^1H$ NOESY, $^1H, ^{15}N$ HSQC experiments respectively. The TOCSY spectra were recorded using the DIPSI pulse sequence with mixing times (spin-lock) of 60–80 ms. The NOESY experiments were acquired with mixing times of 50–100 ms. For reference, NOESY experiments on BN dissolved in PB a NOE mixing time in the range 300–500 ms was used. Spectra were acquired and processed using the TopSpin™ (Bruker Inc, Billerica, MA, US) software. The peptide resonance assignments were obtained using standard strategies based on the 2D NMR experiments.

BN structure calculation. Interactive peak picking using the CARA software (<http://cara.nmr-software.org/portal/>) was exploited to generate the peak lists for NOESY spectra. The NOESY cross-peak volumes were determined using the automated CARA peak integration routine. Conversion of NOE peak intensities to distance restraints was done using automatic calibration as implemented in CYANA 3.98 [34,35]. Prediction of the peptide backbone torsion angles from chemical shifts obtained through TALOS+ [45]. The three-dimensional structures of BN in presence of SDS micelles were determined using the standard protocol of combined automated NOE (nuclear Overhauser effect) assignment and the structure calculation implemented in CYANA. Seven cycles of combined automated NOESY assignment and structure calculations were followed by a final structure calculation. The structure calculation started in each cycle from 200 randomized conformers and the standard simulated annealing schedule was used. The 20 conformers with the lowest final CYANA target function values were retained for analysis and passed to the next cycle.

The Maestro suite [46] as implemented in Schrödinger Release 2016-4 was used to visualize 3D structures.

3.3. Conformational studies on potential GRP-R ligands

Molecular mechanics and dynamics studies were conducted with MacroModel as implemented in Schrödinger Release 2016-4 [40], using AMBER* force field [39]. The starting coordinates for dynamics calculations were those obtained after energy minimization of the structures, followed by conformational search. A systematic variation of the

torsional degrees of freedom of the molecules allowed different starting structures to be constructed that were further minimized to provide the corresponding local minima. For each compound, the conformer with the lowest energy was considered. Simulations were carried out over 5 ns at 298 K with a 0.25 fs time step and a 20 ps equilibration step; 100 structures were sampled and minimized for further analysis. The continuum GB/SA solvent model was employed and the general PRCG (Polak–Ribiere Conjugate Gradient) method for energy minimization was used. An extended cut-off was applied and the SHAKE procedure for bonds was not selected.

3.4. Chemical synthesis

Compounds 1–3 [23] and compound 5 [41] were synthesized according to slightly modified procedures described in literature. The synthesis and characterization, including NMR spectra, of all intermediates, compounds 1–14, are fully reported in [Supplementary materials](#).

Compound 4(R). To a stirred solution of **3** (1.3 g, 5.32 mmol) in anhydrous DMF (10 mL), benzaldehyde dimethyl acetal (927 μ L, 6.38 mmol) and (\pm)-10-Camphorsulfonic acid (CSA) (494 mg, 2.13 mmol) were added under argon atmosphere and the resulting mixture was stirred at 70 $^{\circ}C$ under reduced pressure for 2 h. Then, the reaction was quenched by addition of Et_3N (333 μ L, 2.39 mmol) and the solvent was removed under reduced pressure. The crude was purified by automated flash chromatography (Hex:AcOEt gradient elution) obtaining pure compound **4(R)** as mixture of inseparable diastereoisomers (73:27) at benzylidene function (yellow oil, 830 mg, 44% yield, total recovery 75%). TLC RF = 0.47 (petroleum ether: AcOEt 1:1). 1H NMR (400 MHz, Methanol- d_4) δ 7.58–7.45 (m, 2H, H17, H21), 7.41–7.31 (m, 3H, H18, H19, H20), 5.76 (s, H15 minor isomer), 5.58 (s, 1H, H15), 5.04 (dt, J = 7.5, 4.1 Hz, 1H, 2), 4.74 (d, J = 8.3 Hz, H2 minor isomer), 4.68–4.61 (m, minor isomer), 4.36 (bt, 1H, H3), 4.30 (m, minor isomer), 4.25 (d, J = 12.7 Hz, 1H, H13'), 4.19–4.13 (m, 1H, H13''), 4.08 (dt, J = 10.9, 5.4 Hz, 1H, H10), 4.03 (dd, J = 5.5, 2.1 Hz, H7 minor isomer), 4.00–3.95 (m, 1H, H7), 3.94 (m, H4, H10 minor isomer), 3.88–3.81 (m, 1H, H8), 3.71 (s, 1H, H4), 3.68–3.62 (m, minor isomer), 3.58 (dd, J = 13.2, 3.1 Hz, H12' minor isomer), 3.44 (dd, J = 12.9, 3.4 Hz, 1H, H12' and H12'' minor isomer), 3.33 (m, 1H, H12'' over solvent peak), 2.50 (dt, J = 15.1, 7.8 Hz, H11' minor isomer), 2.31 (dt, J = 14.3, 7.3 Hz, 1H, H11'), 1.94–1.88 (m, H11'' minor isomer), 1.83 (ddd, J = 13.5, 6.9, 3.2 Hz, 1H, H11''). ^{13}C NMR: (100 MHz, Methanol- d_4) δ 139.77 (C16), 138.41 (C16 minor isomer), 130.67, 129.90, 129.17, 129.11, 128.42, 127.45 (Ph), 105.05 (C15 minor isomer), 101.87 (C15), 85.10 (C7), 78.46 (C10), 78.33 (C10 minor isomer), 78.17 (C2), 76.73 (C3), 76.08 (C7 minor isomer), 75.38 (C2 minor isomer), 74.52 (C8), 73.60 (minor isomer), 73.35 (C13), 73.18 (minor isomer), 70.58 (C4 minor isomer), 68.65 (C4), 62.79 (minor isomer), 61.53 (minor isomer), 55.41 (C12), 54.34 (C12 minor isomer), 37.72 (C11 minor isomer), 36.19 (C11). MS (ESI)

calculated for $[C_{16}H_{19}N_3O_5]$ 333.13; found 334.2 $[M + H]^+$, 356.2 $[M + Na]^+$, 351.3 $[M + H_2O + H]^+$.

GRPR-L1. To a stirred solution of **8** (28.3 mg, 0.033 mmol) in anhydrous MeOH (1.7 mL), formic acid (87 μ L) was slowly added at 0 °C and the resulting mixture was heated at 50 °C and stirred for 5 h under argon atmosphere. Then, reaction was quenched by addition of Et₃N (100 μ L) and concentrated under reduced pressure. The crude was purified by automated flash chromatography (AcOEt:MeOH gradient elution) obtaining pure compound **GRPR-L1** (19 mg, 91% yield). TLC RF = 0.27 (AcOEt:MeOH 9:1). ¹H NMR (400 MHz, Chloroform-*d*) δ 8.49 (d, *J* = 8.5 Hz, 1H, Harom), 8.40 (d, *J* = 8.6 Hz, 1H, H14), 8.37 (d, *J* = 8.6 Hz, H14* minor isomer), 8.20 (ddd, *J* = 7.3, 2.8, 1.3 Hz, 1H, Harom), 8.15 (s, 1H, H13), 8.08 (s, minor isomer), 7.58–7.41 (m, 3H, Harom), 7.39–7.31 (m, 3H, CH Ph), 7.31–7.27 (m, 2H, CH Ph), 7.15–7.08 (m, 2H, H12, Harom), 6.98 (s, minor isomer), 5.67 (s, H15* minor isomer), 5.42 (s, 1H, H15), 5.05–4.93 (m, 1H, H1), 4.74 (d, *J* = 12.8 Hz, 1H, H10'), 4.66 (d, *J* = 12.5 Hz, 1H, H10''), 4.55 (d, *J* = 12.6 Hz, H10'* minor isomer), 4.50–4.41 (m, H10''* minor isomer), 4.38 (t, *J* = 2.5 Hz, 1H, H4), 4.23–4.07 (m, 3H, H2, H8, H6''), 3.95 (d, *J* = 12.2 Hz, 1H, H6'), 3.85 (dt, *J* = 5.4, 2.6 Hz, 1H, H3), 3.67 (dt, *J* = 8.6, 4.5 Hz, minor isomer), 3.59 (d, *J* = 5.9 Hz, 1H, H6'* minor isomer), 3.44 (bm, 1H, H5), 3.24 (dd, *J* = 14.2, 4.1 Hz, H9'* minor isomer), 3.08 (qt, *J* = 9.8, 5.4 Hz, 2H, H9), 2.84 (s, 6H, NMe), 2.30 (dt, *J* = 14.7, 7.4 Hz, H7'* minor isomer), 2.07 (td, *J* = 13.4, 12.6, 6.1 Hz, 1H, H7''), 2.00 (d, *J* = 13.6 Hz, H7''* minor isomer), 1.65–1.55 (m, 1H, H7''). ¹³C NMR (100 MHz, CDCl₃) δ 151.95, 151.91 (Cq N), 137.76 (Cq S), 136.64 (Cq), 135.47 (C11), 135.30, 132.42, 131.50, 130.43, 130.29, 130.01, 129.94 (Cq), 129.72 (Cq), 129.68, 129.29, 129.23, 129.05, 128.83, 128.51, 128.42, 128.39, 127.88, 127.45, 126.41, 123.35, 119.42, 119.22, 118.50, 115.40, 115.34, 104.09, 100.81 (C15), 82.68 (C2), 80.17 (C3), 77.66 (C8), 76.54, 75.15, 74.54, 74.28, 72.87 (C4), 72.41 (C6), 72.31, 72.05, 69.98, 67.47, 67.05 (C5), 65.14, 63.64, 61.65 (C10), 47.39 (C9), 45.54 (NMe), 45.13, 36.40, 35.17 (C7). MS (ESI) calculated for $[C_{32}H_{36}N_4O_7S]$ 620.23; found 621.5 $[M + H]^+$, 643.3 $[M + Na]^+$, 655.3 $[M + K]^+$.

GRPR-L2. To a stirred solution of **9** (32 mg, 0.044 mmol) in anhydrous MeOH (1 mL), TFA (1 mL) was slowly added at 0 °C and the resulting mixture was heated at 50 °C and stirred for 5 h under argon atmosphere. Then, reaction was quenched by addition of Et₃N (100 μ L) and concentrated under reduced pressure. The crude was purified by automated flash chromatography (RP18, H₂O:MeOH gradient elution) obtaining pure compound **GRPR-L2** (17 mg, quant % yield). TLC RF = 0.10 (AcOEt:MeOH 7:3). ¹H NMR (400 MHz, Methanol-*d*₄) δ 8.87 (bs, 1H, H13), 7.87–7.79 (m, 2H, Harom), 7.58–7.50 (m, 2H, H12, H14), 7.50–7.40 (m, 3H, Harom), 4.78 (d, *J* = 2.2 Hz, 1H, H10), 4.58 (m, 1H, H1), 4.31–4.20 (m, 1H, H8), 4.17 (bt, 1H, H4), 4.01 (dd, *J* = 10.1, 5.3 Hz, 1H, H2), 3.91–3.76 (m, 2H, H5, H6'), 3.75–3.61 (m, 2H, H3, H6''), 3.57 (ddd, *J* = 21.6, 13.3, 5.2 Hz, 2H, H9), 2.30 (dq, *J* = 14.3, 7.3 Hz, 1H, H7''), 1.89 (m, 1H, H7'). ¹³C NMR (101 MHz, Methanol-*d*₄) δ 170.47 (CO), 135.67 (Cq), 132.74, 132.69 (C12, C14), 132.133 (C11), 129.64, 129.58, 128.24 (Carom), 82.51 (C2), 81.47 (C3), 78.18 (C8), 78.05 (C5), 74.49 (C1), 67.31 (C4), 61.71 (C10), 60.88 (C6), 45.31 (C9), 35.42 (C7). MS (ESI) calculated for $[C_{20}H_{25}N_3O_6]$ 403.17; found 404.1 $[M + H]^+$, 426.1 $[M + Na]^+$.

GRPR-L3. To a stirred solution of **9** (15 mg, 0.02 mmol) in anhydrous MeOH (1 mL), formic acid (54 μ L) was slowly added at 0 °C and the resulting mixture was heated at 50 °C and stirred for 5 h under argon atmosphere. Then, reaction was quenched by addition of Et₃N (100 μ L) and concentrated under reduced pressure. The crude was purified by automated flash chromatography (AcOEt:MeOH gradient elution) obtaining pure compound **GRPR-L3** (10 mg, quant % yield). TLC RF = 0.19 (AcOEt:MeOH 9:1). ¹H NMR (400 MHz, Methanol-*d*₄) δ 8.36 (s, 1H, H13), 7.90 (s, 1H, H14), 7.82 (m, 2H, Harom), 7.56–7.49 (m, 1H, Harom), 7.49–7.39 (m, 5H, Harom), 7.39–7.30 (m, 3H, Harom), 7.17 (s, 1H, H12), 7.09 (s, H12* minor isomer), 5.74 (s, H15* minor isomer), 5.54 (s, 1H, H15), 5.10 (ddd, *J* = 7.1, 4.5, 2.7 Hz, 1H, H1), 4.71 (dd, *J* = 12.8, 2.2 Hz, 2H, H10), 4.64 (dd, *J* = 8.4, 2.5 Hz, minor isomer), 4.51 (t,

J = 2.6 Hz, 1H, H4), 4.42 (d, *J* = 5.3 Hz, H10* minor isomer), 4.26–4.21 (m, 1H, H6'), 4.22–4.16 (m, 1H, H8), 4.13 (dd, *J* = 12.6, 2.2 Hz, 1H, H6''), 4.11–4.05 (m, 1H, H2), 4.02–3.98 (m, minor isomer), 3.81 (dd, *J* = 5.5, 2.1 Hz, 1H, H3), 3.68–3.60 (m, 2H, H5, H9'), 3.54 (dd, *J* = 13.8, 4.2 Hz, 1H, H9''), 2.52 (dt, *J* = 14.9, 7.8 Hz, H7'* minor isomer), 2.38 (dt, *J* = 14.3, 7.4 Hz, 1H, H7''), 1.85 (ddd, *J* = 13.9, 6.2, 2.6 Hz, 1H, H7''). ¹³C NMR (100 MHz, Methanol-*d*₄) δ 170.49 (CO), 139.67 (Cq), 135.81 (Cq), 134.57 (C11), 132.68, 129.97, 129.58, 129.55, 129.19, 129.14, 128.41, 128.38, 128.30, 127.45, 119.98 (C12), 105.09 (C15* minor isomer), 101.80 (C15), 84.33 (C2), 81.52 (C3), 78.60 (C1), 78.51 (C8), 74.05 (C4), 73.52 (C6), 68.79 (C5), 65.59 (C10* minor isomer), 63.57 (C10), 45.22 (C9), 36.76 (C7). MS (ESI) calculated for $[C_{27}H_{29}N_3O_6]$ 491.20; found 492.2 $[M + H]^+$, 514.2 $[M + Na]^+$, 530.2 $[M + K]^+$.

GRPR-L4. To a stirred solution of **10** (26 mg, 0.033 mmol) in anhydrous MeOH (1.5 mL), formic acid (75 μ L) was slowly added at 0 °C and the resulting mixture was heated at 50 °C and stirred for 5 h under argon atmosphere. Then, reaction was quenched by addition of Et₃N (150 μ L) and concentrated under reduced pressure. The crude was purified by automated flash chromatography (AcOEt:MeOH gradient elution) obtaining pure compound **GRPR-L4** (16.4 mg, 92% yield). TLC RF = 0.15 (AcOEt:MeOH 9:1). ¹H NMR (400 MHz, Methanol-*d*₄) δ 8.34 (s, 1H, H14), 8.08 (s, 1H, H12), 7.78–7.65 (m, 2H, Harom), 7.55–7.49 (m, 1H, minor isomer), 7.48–7.40 (m, 2H, Harom), 7.35 (m, 4H, Harom), 6.80–6.63 (m, 2H, Harom), 5.74 (s, H15* minor isomer), 5.54 (s, 1H, H15), 5.17–4.99 (m, 1H, H1), 4.72 (s, 2H, H10), 4.54–4.49 (m, 1H, H4), 4.47–4.34 (m, H10* minor isomer), 4.29–4.21 (m, 1H, H6'), 4.15 (m, 2H, H6'', H8), 4.08 (t, *J* = 4.5 Hz, 1H, H2), 4.03–3.90 (m, minor isomer), 3.80 (d, *J* = 5.4 Hz, 1H, H3), 3.67–3.63 (m, 1H, H5), 3.62–3.56 (m, 1H, H9''), 3.56–3.49 (m, 1H, H9'), 3.01 (s, 6H, NMe), 2.99 (s, NMe, minor isomer), 2.50 (dt, *J* = 14.8, 7.8 Hz, H7'* minor isomer), 2.43–2.29 (m, 1H, H7''), 1.84 (dd, *J* = 14.7, 10.2 Hz, 1H, H7''). ¹³C NMR (100 MHz, CD₃OD) δ 170.66, 170.59 (CO), 154.27, 154.24, 139.66, 138.38, 130.70, 130.49, 129.98, 129.88, 129.76, 129.19, 129.15, 128.40, 127.45, 121.94, 121.69, 119.84, 112.18, 112.11, 112.07, 105.08, 101.81 (C15), 84.08 (C2), 81.64 (C3), 78.70 (C8), 78.57 (C1), 78.45, 75.84, 75.62, 74.04 (C4), 73.60, 73.48 (C6), 73.32, 70.77, 68.76 (C5), 68.73, 65.14, 63.13 (C10), 45.08 (C9), 43.34, 40.24, 40.23 (NMe), 38.13, 36.69 (C7). MS (ESI) calculated for $[C_{29}H_{34}N_4O_6]$ 534.25; found 535.2 $[M + H]^+$, 557.2 $[M + Na]^+$.

GRPR-L5. To a stirred solution of **11** (26 mg, 0.33 mmol) in anhydrous MeOH (1.6 mL), formic acid (75 μ L) was slowly added at 0 °C and the resulting mixture was heated at 50 °C and stirred for 5 h under argon atmosphere. Then, reaction was quenched by addition of Et₃N (100 μ L) and concentrated under reduced pressure. The crude was purified by automated flash chromatography (AcOEt:MeOH gradient elution) obtaining pure compound **GRPR-L5** (13 mg, 83% yield). TLC RF = 0.16 (AcOEt:MeOH 9:1). ¹H NMR (400 MHz, Chloroform-*d*) δ 7.87–7.76 (m, 3H, Harom), 7.58–7.48 (m, 1H, H14), 7.45–7.29 (m, 5H, Harom), 7.01 (s, 1H, H12), 6.87 (m, 2H, Harom), 5.74 (s, minor isomer), 5.46 (s, 1H, H15), 5.13 (ddd, *J* = 6.7, 4.3, 2.1 Hz, 1H, H1), 4.71 (dd, *J* = 13.3, 9.2 Hz, 2H, H10), 4.66–4.56 (m, minor isomer), 4.50 (d, *J* = 12.4 Hz, minor isomer), 4.42–4.37 (m, 1H, H4), 4.31 (m, 2H, H8, H6'), 4.23 (dd, *J* = 8.3, 1.7 Hz, minor isomer), 4.13 (t, *J* = 4.9 Hz, 1H, H2), 4.05 (dd, *J* = 12.9, 2.2 Hz, 1H, H6''), 4.01–3.87 (m, minor isomer), 3.80 (s, 1H, minor isomer), 3.79 (s, 3H, OMe), 3.78–3.69 (m, 2H, H3, H9''), 3.63–3.55 (m, 1H, H9'), 3.53 (s, 1H, H5), 2.50 (dt, *J* = 15.1, 8.1 Hz, minor isomer), 2.37 (dq, *J* = 15.2, 7.6 Hz, 1H, H7''), 1.92–1.76 (m, 1H, H7'). ¹³C NMR (100 MHz, CDCl₃) δ 167.92 (CO), 167.81, 162.42, 162.25 (Cq), 137.78 (Cq), 136.54 (C11), 130.09, 129.34, 129.13, 129.08, 128.56, 128.46, 127.45, 126.79 (Cq), 126.43, 126.37, 113.87, 113.79, 104.20, 100.84 (C15), 83.34 (C2), 79.59 (C3), 77.77 (C8), 77.51 (C1), 76.98, 74.76, 74.15, 72.97, 72.68 (C6), 72.28, 72.18, 69.95, 67.92, 67.54 (C5), 64.52, 61.92 (C10), 55.56, 55.54 (OMe), 44.02 (C9), 43.18, 37.72, 35.95 (C7). MS (ESI) calculated for $[C_{28}H_{31}N_3O_7]$ 521.22; found 522.2 $[M + H]^+$, 544.3 $[M + Na]^+$.

GRPR-L6. To a stirred solution of **12** (30 mg, 0.053 mmol) in freshly degassed MeOH (2.7 mL), a catalytic amount of Pd/CaCO₃ (Lindlar's catalyst) was added, then the mixture was stirred under H₂ atmosphere at r.t. for 2 h. The crude was diluted with MeOH and the catalyst was filtered off through a celite pad. Removal of the solvent under reduced pressure afforded pure amine in a quantitative yield that was immediately used. Amine derivative was resuspended in anhydrous DCM (1.4 mL), benzoyl-chloride (12 µL, 0.106 mmol) and Et₃N (22 µL, 0.159 mmol) were added at 0 °C. The mixture was allowed to return to room temperature and stirred under argon atmosphere overnight. Then, the reaction was quenched with MeOH and concentrated under reduced pressure and the crude was purified by automated flash chromatography (Hex:AcOEt gradient elution) obtaining pure compound **GRPR-L6** (30 mg, 89% yield). TLC RF = 0.59 (EDP:AcOEt 1:1). ¹H NMR (400 MHz, Chloroform-d) δ 7.86 (s, 1H, Harom), 7.83–7.73 (m, 3H, Harom), 7.61–7.30 (m, 8H, Harom), 6.76 (t, *J* = 5.2 Hz, 1H, NH), 6.62–6.51 (m, minor isomer), 5.79 (s, minor isomer), 5.55 (s, 1H, H15), 5.19 (ddd, *J* = 6.5, 3.9, 1.8 Hz, 1H, H1), 4.90 (d, *J* = 13.1 Hz, 1H, H10'), 4.84–4.75 (m, 1H, H10''), 4.68 (dd, *J* = 8.2, 2.5 Hz, minor isomer), 4.65–4.54 (m, minor isomer), 4.51 (t, *J* = 2.6 Hz, 1H, H4), 4.38 (d, *J* = 12.7 Hz, 1H, H6'), 4.33 (dd, *J* = 8.2, 1.8 Hz, minor isomer), 4.27 (dtd, *J* = 8.7, 5.7, 3.0 Hz, 1H, H8), 4.17 (t, *J* = 4.4 Hz, 1H, H2), 4.12 (dd, *J* = 12.8, 2.2 Hz, 1H, H6''), 4.04 (ddt, *J* = 12.8, 7.1, 3.3 Hz, minor isomer), 4.00–3.90 (m, minor isomer), 3.83–3.67 (m, 2H, H3, H9''), 3.67–3.63 (m, minor isomer), 3.63–3.55 (m, 2H, H5, H9'), 3.50 (ddd, *J* = 13.7, 7.6, 4.5 Hz), 2.60 (dt, *J* = 14.7, 7.6 Hz, minor isomer), 2.44 (ddd, *J* = 14.8, 8.4, 6.8 Hz, 1H, H7'), 1.87 (ddd, *J* = 14.5, 6.0, 2.0 Hz, 1H, H7''), 1.84–1.76 (m, minor isomer). ¹³C NMR (100 MHz, CDCl₃) δ 168.03 (Cq), 167.70, 141.04, 140.92, 137.66, 136.49, 134.89, 134.29, 133.50, 131.84, 131.80, 131.75, 131.56, 131.51, 131.47, 130.16, 130.09, 129.32, 128.75, 128.69, 128.62, 128.56, 128.54, 128.52, 128.46, 127.61, 127.57, 127.43, 127.32, 127.08, 127.00, 126.24, 104.29, 100.68 (C15), 83.51 (C2), 81.14 (C3), 77.60 (C1), 77.29, 77.19 (C8), 74.80, 74.17, 72.79 (C4), 72.69 (C6), 72.23, 71.97, 71.95, 70.39, 69.58 (C10), 67.84, 67.69 (C5). MS (ESI) calculated for [C₃₂H₂₉F₆NO₆] 637.19; found 638.28 [M + H]⁺, 660.24 [M + Na]⁺, 676.26 [M + K]⁺.

GRPR-L7. To a stirred solution of **13** (26 mg, 0.057 mmol) in freshly degassed MeOH (2.9 mL), a catalytic amount of Pd/CaCO₃ (Lindlar's catalyst) was added, then the mixture was stirred under H₂ atmosphere at r.t. for 2 h. The crude was diluted with MeOH and the catalyst was filtered off through a celite pad. Removal of the solvent under reduced pressure afforded pure amine in a quantitative yield that was immediately used. Amine derivative was resuspended in anhydrous DCM (1.45 mL), benzoyl-chloride (13 µL, 0.114 mmol) and Et₃N (24 µL, 0.171 mmol) were added at 0 °C. The mixture was allowed to return to room temperature and stirred under argon atmosphere overnight. Then, the reaction was quenched with MeOH and concentrated under reduced pressure and the crude was purified by automated flash chromatography (Hex:AcOEt gradient elution) obtaining pure compound **GRPR-L7** (27 mg, 87% yield). TLC RF = 0.38 (EDP:AcOEt 4:6). ¹H NMR (400 MHz, Chloroform-d) δ 8.17–8.04 (m, minor isomer), 7.87–7.71 (m, 2H, Harom), 7.65–7.34 (m, 9H, Harom), 7.32 (qAB, *J* = 8.5 Hz, 1H, Harom), 7.22 (d, *J* = 8.5 Hz, minor isomer), 6.88–6.80 (qAB, 2H, Harom), 6.58 (t, *J* = 5.6 Hz, NH), 5.79 (s, H15* minor isomer), 5.49 (s, 1H, H15), 5.16 (ddd, *J* = 6.3, 4.0, 1.7 Hz, 1H, H1), 4.76 (d, *J* = 11.8 Hz, 1H, H10'), 4.64 (d, *J* = 12.0 Hz, 1H, H10''), 4.49 (d, *J* = 11.7 Hz, 10''* minor isomer), 4.40 (d, *J* = 11.8 Hz, 10''* minor isomer), 4.37 (t, *J* = 2.6 Hz, 1H, H4), 4.35–4.24 (m, 2H, H8, H6''), 4.16 (t, *J* = 4.3 Hz, 1H, H2), 4.05 (dd, *J* = 12.7, 2.1 Hz, 1H, H6'), 4.01–3.95 (m, minor isomer), 3.82 (dd, *J* = 5.4, 3.1 Hz, 1H, H9''), 3.79 (s, minor isomer), 3.75 (s, 3H, OMe), 3.63 (dt, *J* = 4.7, 2.4 Hz, 1H, H3), 3.60–3.51 (m, 1H, H9'), 3.49 (d, *J* = 3.7 Hz, 1H, H5), 2.55 (dt, *J* = 14.9, 7.7 Hz, H7'* minor isomer), 2.41 (ddd, *J* = 14.8, 8.5, 6.8 Hz, 1H, H7'), 1.86 (ddd, *J* = 14.3, 5.5, 1.8 Hz, 1H, H7''), 1.82–1.76 (m, H7''* minor isomer). ¹³C NMR (100 MHz, CDCl₃) δ 167.87 (CO), 167.61(*), 159.25 (Cq), 159.14 (*), 137.71 (Cq), 136.54 (*), 134.85 (Cq), 134.23 (*), 133.44, 131.58, 131.34 (CHarom), 130.20

(Cq), 130.09, 129.87, 129.65, 129.56 (CHarom), 129.54 (*), 129.39, 129.33, 129.09, 128.99, 128.59, 128.53, 128.47, 128.41, 128.39, 128.25, 127.34, 126.98, 126.93, 126.90, 126.25 (CH arom), 113.75 (CH arom AB), 113.71 (*), 104.03 (*), 100.66 (C15), 83.75 (C2), 79.04 (C3), 77.44 (C1), 76.73 (C8), 74.85, 73.90, 73.17 (*), 73.03 (C4), 72.51 (C6), 72.10, 71.98, 70.45 (C10), 69.22 (*), 67.80, 67.54 (C5), 55.26, 55.23 (OMe), 43.93 (C9), 43.15 (*), 37.25 (*), 35.63 (C7). MS (ESI) calculated for [C₃₁H₃₃NO₇] 531.22; found 532.14 [M + H]⁺, 554.20 [M + Na]⁺, 570.15 [M + K]⁺.

3.5. Cell cultures

PC3 and MCF-7 cell lines were obtained from ATCC. PC-3 cells were cultured in RPMI 1640 w/Glutamine supplemented with 10% (v/v) fetal bovine serum (FBS), 100 U/mL penicillin, 100 µg/mL streptomycin (all from Euroclone SpA, Pero, Italy). MCF-7 cells were cultured in EMEM/NEAA supplemented with 10% (v/v) FBS, 2 mM L-glutamine, 100 U/mL penicillin, 100 µg/mL streptomycin (all from Euroclone SpA, Pero, Italy). Both cell lines were maintained at 37 °C in a humidified 5% CO₂ incubator.

3.6. Calcium mobilization assay

Calcium mobilization was evaluated using the FLUO-4 Calcium Assay kit (ThermoFisher Scientific, Waltham, MA, US, cat # F36206) according to manufacturer's instruction. The assay was performed using a BMG OmegaStar (LabTech, Sorisole, BG, Italy) multiplate reader equipped with a dual automatic injection system and fluorescence instrument settings appropriate for excitation at 494 nm and emission at 516 nm. The assay chamber was maintained at 37 °C for the whole experiment duration. Briefly, PC3 cells were plated 4x10⁴ cells/well in 96-well dark plates with transparent bottom. The next day, after removing the culture medium, 100 µL/well dye loading solution was added and incubated for 45 min at 37 °C in the dark. The plate was transferred into the multiplate reader assay chamber. Using the automatic injection system GRPR-L diluted in assay buffer was added to each well to obtain a final concentration of 50 nM; fluorescence (F) was acquired in each well every second for 20 s just prior to compound injection and for 60 s after injection. Mean fluorescence prior compound injection was used as reference (F₀) for signal normalization (F/F₀). After 30 min using the automatic injection system, BN dissolved in assay buffer was added (well concentration 200 nM) and fluorescence was acquired as described above to monitor intracellular Ca²⁺ mobilization. Samples not pre-treated with any GRPR-L and stimulated only with Bombesin 200 nM were also assayed. Cells treated with assay buffer only represented the negative control.

3.7. PC3 cell proliferation assays

To assess the effect of the different GRPR-L compounds on PC3 cell proliferation, the SRB (SulfoRhodamine B) assay was performed. PC3 cells were seeded 5000/well in 96-wells plate in complete medium, consisting of RPMI 1640 w/Glutamine supplemented with antibiotics and 10% Fetal Bovine Serum (FBS) (all from Euroclone). The day after, the complete medium was replaced with RPMI 1640 w/Glutamine supplemented with antibiotics without serum. After 36–48 h of serum starvation, cells were treated with 50 nM of GRPR-L compounds in complete medium for 1 h and subsequently BN was added to reach a final concentration of 200 nM; samples not treated with BN received the same amount of medium. Controls were treated with complete medium without any drug. A BN control (cells treated with BN only) was also performed. After 24 h of GRPR-L induction, 50 µL of 50% Trichloroacetic acid (TCA) was added to each well and the plate was incubated for 1 h at 4 °C. Plate was rinsed with tap water and allowed to dry at room temperature. SRB solution (0.4% SRB in TCA 1%) was added (50 µL/well) and incubated for 15 min. Excess dye was rinsed thoroughly with

TCA 1% and the plate was allowed to dry at room temperature. SRB was solubilized with Tris(Hydroxymethyl)aminomethane 10 mM 150 μ L/well and optical density at 540 nm was measured using a multiplate reader (OmegaStar, BMG Labtech, Germany). To account for unspecific staining, wells without cells but containing medium for the entire experimental period were also assayed and the value obtained was subtracted as background. Proliferation was calculated as ratio versus control untreated cells. Three independent experiments were conducted, each with six replicates.

3.8. MCF-7 cell proliferation assays

The activity of the GRPR-L compounds on MCF-7 proliferation was measured by the 3-(4,5-dimethylthiazol-2-yl)-2,5-diphenyltetrazolium bromide (MTT) assay. 4000 cells/well were seeded in 96-well plates. The day after, the complete medium was replaced with EMEM-serum free medium containing 0.1% BSA (Merck KGaA, Darmstadt, Germany). After 24 h starvation, GRPR-L compounds were added at the indicated concentrations from 1000X stocks in 100% DMSO, in the presence or absence of 100 nM BN to stimulate proliferation; 0.1% DMSO was added in the solvent control wells. After 24 h treatment, the MTT solution (Merck, used at a final concentration of 0.5 mg/ml) was added and plates were incubated for 2 h at 37 °C. The purple formazan crystals were solubilized, and the plates were read on a Victor X3 Microplate Reader (Perkin Elmer inc., Waltham, MA, US) at 570 nm. Growth of each condition was referred to solvent control, which was set to 100%. All conditions were tested at least in three independent experiments, all in technical triplicates. Wells without cells but containing medium for the entire experimental period were also assayed and the value obtained was subtracted as background. Proliferation was calculated as ratio versus control untreated cells.

4. Conclusions

Here we combined CD, NMR and MM/MD-based conformational studies, organic synthesis and *in vitro* cellular assays to develop a new small library of GRP-R ligands based on a rigid bicyclic C-galactosidic scaffold.

Collectively, our results clearly indicate that we obtained new non-peptide GRP-R high affinity ligands, some of which show a significant BN antagonist activity. To the best of our knowledge, our compounds are the only example of a small library of non-peptide GRP-R antagonists active in the nM range of concentration, with the only exception of compound PD176252, that, as already mentioned, shows poor selectivity for GRP-R [20,21],

These molecules are hit compounds for the rational design and synthesis of new ligands and modulators of GRP-R. Due to their favorable chemical properties and stability, they can be used for the active receptor-mediated targeting of GRP-R positive tumors.

To give specific examples, the presence of free hydroxyl groups on compound **GRPR-L2** can be exploited to enable its chemical conjugation to radiolabeled compounds for selective anti-tumor radiotherapy and/or imaging, or well-characterized and potent anti-cancer agents, obtaining very efficient molecular devices for drug targeting of tumor tissues. Moreover, the bioactivity of compounds **GRPR-L6**, bearing a 3,5-bis-(trifluoromethyl) phenyl group, suggests the possibility to synthesize 18 F-labeled GRPR-L as potential PET agents for the imaging of GRP-R positive tumors.

These new strategies, assuming the development of specific synthetic approaches for the preparation of new derivatives and conjugates, will be explored by our group in the near future.

Declaration of Competing Interest

The authors declare that they have no known competing financial interests or personal relationships that could have appeared to influence

the work reported in this paper.

Acknowledgments

The authors acknowledge AIRC for funding My First AIRC project 17030 - Targeting of Gastrin-Releasing Peptide receptor expressing tumors: NMR characterization of Bombesin/GRP-R interaction.

Authors thanks Prof. Antonino Natalello (Dept of Biotechnology and Biosciences, University of Milano – Bicocca) for helpful discussion of CD data.

Appendix A. Supplementary material

Supplementary data to this article can be found online at <https://doi.org/10.1016/j.bioorg.2021.104739>.

References

- [1] D. Pooja, A. Gunukula, N. Gupta, D.J. Adams, H. Kulhari, Bombesin receptors as potential targets for anticancer drug delivery and imaging, *Int. J. Biochem. Cell Biol.* 114 (2019) 105567.
- [2] T.W. Moody, Peptide receptors as cancer drug targets, *Ann. N. Y. Acad. Sci.* 1455 (1) (2019) 141–148.
- [3] T.J. Stott Reynolds, C.J. Smith, M.R. Lewis, Peptide-based radiopharmaceuticals for molecular imaging of prostate cancer, in: H. Schatten (Ed.), *Advances in Experimental Medicine and Biology*, Springer International Publishing, 2018, pp. 135–158.
- [4] A. Nagy, A.V. Schally, G. Halmos, P. Armatis, R.Z. Cai, V. Csernec, M. Kovács, M. Koppán, K. Szepesházi, Z. Káhn, Synthesis and biological evaluation of cytotoxic analogs of somatostatin containing doxorubicin or its intensely potent derivative, 2-pyrrolinodoxorubicin, *PNAS* 95 (4) (1998) 1794–1799.
- [5] H. Zia, T. Hida, S. Jakowlew, M. Birrer, Y. Gozes, J.C. Reubi, M. Fridkin, I. Gozes, T.W. Moody, Breast cancer growth is inhibited by vasoactive intestinal peptide (VIP) hybrid, a synthetic VIP receptor antagonist, *Cancer Res.* 56 (15) (1996) 3486–3489.
- [6] T.W. Moody, I. Ramos-Alvarez, R.T. Jensen, Neuropeptide G protein-coupled receptors as oncotargets, *Front. Endocrinol.* 9 (345) (2018).
- [7] T.J. McDonald, H. Jörnvall, G. Nilsson, M. Vagne, M. Ghatei, S.R. Bloom, V. Mutt, Characterization of a gastrin releasing peptide from porcine non-antral gastric tissue, *Biochem. Biophys. Res. Commun.* 90 (1) (1979) 227–233.
- [8] E. Rozengurt, Signal transduction pathways in the mitogenic response to G protein-coupled neuropeptide receptor agonists, *J. Cell. Physiol.* 177 (4) (1998) 507–517.
- [9] A.G. Aprikian, K. Han, S. Chevalier, M. Bazinet, J. Viallet, Bombesin specifically induces intracellular calcium mobilization via gastrin-releasing peptide receptors in human prostate cancer cells, *J. Mol. Endocrinol.* 16 (3) (1996) 297.
- [10] M. Pagé, Tumor targeting in cancer therapy, *Springer Science & Business Media*, 2002.
- [11] J.C. Reubi, Peptide receptors as molecular targets for cancer diagnosis and therapy, *Endocr. Rev.* 24 (4) (2003) 389–427.
- [12] S.M. Okarvi, Peptide-based radiopharmaceuticals and cytotoxic conjugates: Potential tools against cancer, *Cancer Treat. Rev.* 34 (1) (2008) 13–26.
- [13] E.F. Grady, L.W. Slice, W.O. Brant, J.H. Walsh, D.G. Payan, N.W. Bunnett, Direct observation of endocytosis of gastrin releasing peptide and its receptor, *J. Biol. Chem.* 270 (9) (1995) 4603–4611.
- [14] A. Accardo, R. Mansi, G. Salzano, A. Morisco, M. Aurilio, A. Parisi, F. Maione, C. Cicala, B. Ziaco, D. Tesaro, L. Aloj, G. De Rosa, G. Morelli, Bombesin peptide antagonist for target-selective delivery of liposomal doxorubicin on cancer cells, *J. Drug Target.* 21 (3) (2013) 240–249.
- [15] R. Cescato, T. Maina, B. Nock, A. Nikolopoulou, D. Charalambidis, V. Piccand, J. C. Reubi, Bombesin receptor antagonists may be preferable to agonists for tumor targeting, *J. Nucl. Med.: Off. Publ. Soc. Nucl. Med.* 49 (2) (2008) 318–326.
- [16] K. Abiraj, R. Mansi, M.L. Tamma, M. Fani, F. Forrer, G. Nicolas, R. Cescato, J. C. Reubi, H.R. Maecke, Bombesin antagonist-based radioligands for translational nuclear imaging of gastrin-releasing peptide receptor-positive tumors, *J. Nucl. Med.: Off. Publ. Soc. Nucl. Med.* 52 (12) (2011) 1970–1978.
- [17] C. Kroll, R. Mansi, F. Braun, S. Dobitz, H.R. Maecke, H. Wennemers, Hybrid bombesin analogues: combining an agonist and an antagonist in defined distances for optimized tumor targeting, *J. Am. Chem. Soc.* 135 (45) (2013) 16793–16796.
- [18] Z. Heidari, R. Sariri, M. Salouti, Gold nanorods-bombesin conjugate as a potential targeted imaging agent for detection of breast cancer, *J. Photochem. Photobiol., B* 130 (2014) 40–46.
- [19] M. Pourghiasian, Z. Liu, J. Pan, Z. Zhang, N. Colpo, K.S. Lin, D.M. Perrin, F. Bénard, (18)F-AmBF3-MJ9: a novel radiofluorinated bombesin derivative for prostate cancer imaging, *Bioorg. Med. Chem.* 23 (7) (2015) 1500–1506.
- [20] V. Ashwood, V. Brownhill, M. Higginbottom, D.C. Horwell, J. Hughes, R. A. Lewthwaite, A.T. McKnight, R.D. Pinnock, M.C. Pritchard, N. Suman-Chauhan, C. Webb, S.C. Williams, PD 176252—the first high affinity non-peptide gastrin-releasing peptide (BB2) receptor antagonist, *Bioorg. Med. Chem. Lett.* 8 (18) (1998) 2589–2594.

- [21] E. Lacivita, E. Lucente, C. Kwizera, I.F. Antunes, M. Niso, P. De Giorgio, R. Perrone, N.A. Colabufo, P.H. Elsinga, M. Leopoldo, Structure-activity relationship study towards non-peptidic positron emission tomography (PET) radiotracer for gastrin releasing peptide receptors: Development of [(18)F] (S)-3-(1H-indol-3-yl)-N-[1-[5-(2-fluoroethoxy)pyridin-2-yl]cyclohexylmethyl]-2-methyl-2-[3-(4-nitrophenyl)ureido]propionamide, *Bioorg. Med. Chem.* 25 (1) (2017) 277–292.
- [22] A. Palmioli, C. Ceresa, F. Tripodi, B. La Ferla, G. Nicolini, C. Airoldi, On-cell saturation transfer difference NMR study of Bombesin binding to GRP receptor, *Bioorg. Chem.* 99 (2020) 103861.
- [23] S. Mari, F.J. Cañada, J. Jiménez-Barbero, A. Bernardi, G. Marcou, I. Motto, I. Velter, F. Nicotra, B. La Ferla, Synthesis and conformational analysis of galactose-derived bicyclic scaffolds, *Eur. J. Org. Chem.* 2006 (13) (2006) 2925–2933.
- [24] U. Hunger, J. Ohnsmann, H. Kunz, Carbohydrate scaffolds for combinatorial syntheses that allow selective deprotection of all four positions independent of the sequence, *Angew. Chem. Int. Ed. Engl.* 43 (9) (2004) 1104–1107.
- [25] F. Nicotra, L. Cipolla, B. La Ferla, C. Airoldi, C. Zona, A. Orsato, N. Shaikh, L. Russo, Carbohydrate scaffolds in chemical genetic studies, *J. Biotechnol.* 144 (3) (2009) 234–241.
- [26] L. Cipolla, B. La Ferla, C. Airoldi, C. Zona, A. Orsato, N. Shaikh, L. Russo, F. Nicotra, Carbohydrate mimetics and scaffolds: sweet spots in medicinal chemistry, *Future Med. Chem.* 2 (4) (2010) 587–599.
- [27] J.A. Carver, The conformation of bombesin in solution as determined by two-dimensional 1H-NMR techniques, *Eur. J. Biochem.* 168 (1) (1987) 193–199.
- [28] M.D. Díaz, M. Fioroni, K. Burger, S. Berger, Evidence of complete hydrophobic coating of bombesin by trifluoroethanol in aqueous solution: an NMR spectroscopic and molecular dynamics study, *Chem. – Eur. J.* 8 (7) (2002) 1663–1669.
- [29] P. Cavatorta, G. Farruggia, L. Masotti, G. Sartor, A.G. Szabo, Conformational flexibility of the hormonal peptide bombesin and its interaction with lipids, *Biochem. Biophys. Res. Commun.* 141 (1) (1986) 99–105.
- [30] P. Cavatorta, A. Spisni, A.G. Szabo, G. Farruggia, L. Franzoni, L. Masotti, Conformation of bombesin in buffer and in the presence of lysolecithin micelles: Nmr, CD, and fluorescence studies, *Biopolymers* 28 (1) (1989) 441–463.
- [31] D.E. Warschawski, A.A. Arnold, M. Beaugrand, A. Gravel, É. Chartrand, I. Marcotte, Choosing membrane mimetics for NMR structural studies of transmembrane proteins, *Biochim. Biophys. Acta (BBA) – Biomembr.* 1808 (8) (2011) 1957–1974.
- [32] M. Adrover, P. Sanchis, B. Vilanova, K. Pauwels, G. Martorell, J.J. Pérez, Conformational ensembles of neuromedin C reveal a progressive coil-helix transition within a binding-induced folding mechanism, *RSC Adv.* 5 (101) (2015) 83074–83088.
- [33] S.M. Kelly, N.C. Price, The application of circular dichroism to studies of protein folding and unfolding, *Biochim. Biophys. Acta (BBA) - Protein Struct. Mol. Enzymol.* 1338 (2) (1997) 161–185.
- [34] P. Güntert, C. Mumenthaler, K. Wüthrich, Torsion angle dynamics for NMR structure calculation with the new program Dyana1 Edited by P. E. Wright, *J. Mol. Biol.* 273 (1) (1997) 283–298.
- [35] P. Güntert, Automated NMR structure calculation With CYANA, in: A.K. Downing (Ed.), *Protein NMR Techniques*, Humana Press, Totowa, NJ, 2004, pp. 353–378.
- [36] A. Palmioli, C. Airoldi, Bombesin structure in presence of SDS micelles, *Mendeley Data*, v1 (2019), doi: 10.17632/sg5fcrnk9z.1.
- [37] H. Ohki-Hamazaki, M. Iwabuchi, F. Maekawa, Development and function of bombesin-like peptides and their receptors, *Int. J. Dev. Biol.* 49 (2–3) (2005) 293–300.
- [38] C. Airoldi, A. Palmioli, Synthesis of C- and S-glycosides, reference module in chemistry, *Molecular Sciences and Chemical Engineering*, Elsevier, 2020.
- [39] J. Wang, R.M. Wolf, J.W. Caldwell, P.A. Kollman, D.A. Case, Development and testing of a general amber force field, *J. Comput. Chem.* 25 (9) (2004) 1157–1174.
- [40] MacroModel, Schrödinger Release 2016-4, Schrödinger, LLC, New York, NY, Schrödinger Release 2016-4, Schrödinger, LLC, New York, NY, 2016.
- [41] H. Peng, D. Carrico, V. Thai, M. Blaskovich, C. Bucher, E.E. Pusateri, S.M. Sebti, A. D. Hamilton, Synthesis and evaluation of potent, highly-selective, 3-aryl-piperazine inhibitors of protein geranylgeranyltransferase-I, *Org. Biomol. Chem.* 4 (9) (2006) 1768–1784.
- [42] W.J. Wasilenko, J. Cooper, A.J. Palad, K.D. Somers, P.F. Blackmore, J.S. Rhim, G. L. Wright Jr., P.F. Schellhammer, Calcium signaling in prostate cancer cells: evidence for multiple receptors and enhanced sensitivity to bombesin/GRP, *Prostate* 30 (3) (1997) 167–173.
- [43] H. Reile, P.E. Armatis, A.V. Schally, Characterization of high-affinity receptors for bombesin/gastrin releasing peptide on the human prostate cancer cell lines PC-3 and DU-145: internalization of receptor bound 125I-(Tyr4) bombesin by tumor cells, *Prostate* 25 (1) (1994) 29–38.
- [44] M. Gugger, J.C. Reubi, Gastrin-releasing peptide receptors in non-neoplastic and neoplastic human breast, *Am. J. Pathol.* 155 (6) (1999) 2067–2076.
- [45] Y. Shen, F. Delaglio, G. Cornilescu, A. Bax, TALOS+: a hybrid method for predicting protein backbone torsion angles from NMR chemical shifts, *J. Biomol. NMR* 44 (4) (2009) 213–223.
- [46] Maestro, Schrödinger Release 2016-4, Schrödinger, LLC, New York, NY, Schrödinger Release 2016-4, Schrödinger, LLC, New York, NY, 2016.